Time–frequency analysis of automotive engine performance via short-time Fourier transform

Zhengmao Ye[1], Radian Belu[1], Hang Yin[1] and Habib Mohamadian[1]

[1] College of Engineering, Southern University, Baton Rouge, LA 70813, USA

Abstract

Electronic control of automotive engines for passenger vehicles has been broadly implemented in order to enhance the overall engine performance. Typical engine control systems include the air/fuel ratio control system, fuel injection control system, ignition control system, idle speed control system, emission aftertreatment system, exhaust gas recirculation control system, and so on. Time domain analysis of engine performances has been well conducted in terms of fuel economy, idle speed stability, and exhaust emissions. However, frequency domain analysis of various engine performances is still in infancy. In this preliminary study, time–frequency analysis of automotive engine performances has been proposed. The time-varying short-time Fourier transform (STFT) can perform fundamental frequency analysis, which has been successfully applied to various fields, such as the spectral envelope extraction, speech modeling, music analysis, time scaling, frequency scaling, fast Fourier transform (FFT) filter banks, and so on. Thus STFT analysis has been formulated to examine the engine performances in the frequency domain analysis. Several case studies are conducted with respect to engine performances on idle speed stability, air/fuel ratio and exhaust emissions. STFT also has potentials to be extended to conduct any other automotive engine performance analyses.

Keywords

Time–frequency analysis, idle speed control (ISC), air/fuel (A/F) ratio control, exhaust emissions, short-time Fourier transform (STFT)

1. Introduction

Both short-time Fourier transform (STFT) and wavelet transforms are broadly applied in engineering and science. STFT uses the sum of complex exponentials to represent signals, which leads to a systematic analysis and synthesis methodology. Meanwhile it could manifest the latent and obscure signal properties beyond the straightforward time domain analysis. There are numerous recent real world applications of STFT. The STFT estimator of Micro-Doppler parameters has been proposed. It outperforms the existing algorithms which can reach the Cramer-Rao lower bound of the frequency-modulated signal parameters. The Micro-Doppler signature can also be applied to the UAV rotor blade analysis [1-2]. Electrification of future warships could be unavoidable, thus time-frequency feature extraction is necessary. The clustering based approach has been applied to extract unique features via STFT analysis under various pulsed loads, so as to further identify the load transient events as well as shunt faults and series arcing faults [3]. The low-complexity adaptive STFT in terms of the chirp rate has been introduced. It shows superiority over other schemes in low signal-to-noise ratio (SNR) environments on the instantaneous frequency estimation. At the same time, Principal Component Analysis (PCA) is used to replace the difference operator to enhance robustness in calculating [4]. A STFT based blind source separation algorithm is designed for separating closely spaced multipath signals under Gaussian noises. It aims to compensate for the multipath effect and complex noise in practical wireless communication systems. It performs the better separation of multipath signals [5]. The spatio-temporal STFT block is proposed to simplify the computational complexity and improve

IVUS 2022: 27th International Conference on Information Technology, May 12, 2022, Kaunas, Lithuania
EMAIL: zhengmao_ye@subr.edu (Z. Ye); radian_belu@subr.edu (R. Belu); hang_yin@subr.edu (H. Yin); habib_mohamadian@subr.edu (H. Mohamadian)
ORCID: 0000-0001-8897-574X (Z. Ye); 0000-0002-5892-3225 (R. Belu); 0000-0002-4600-5881 (H. Yin); 0000-0002-2099-2292 (H. Mohamadian)

the learning capability of classical 3D convolutional neural networks via a STFT kernel at the low frequency nodes. With fewer parameters and lower costs, it provides better performance than some other state-of-the-art methods [6]. Time-frequency analysis is applied to industrial applications of system-on-chip design, where the startup transient current and voltage supply to the induction motor as well as robot link vibration signals are well monitored. Both STFT and Discrete Wavelet Transform (DWT) are suitable to early abnormality diagnosis [7]. DWT is another practical approach to solve complex nonlinear problems. Essentially it is designed to conduct analysis between the time domain and frequency domain, however it can also be easily extended to spatial domain analysis. Some case studies in time domain, frequency domain, and spatial domain are conducted, where integration of DWT and Nonlinear Component Analysis (NCA) has been applied for discrete wavelet denoising with satisfied results [8].

Automotive engine control is an important and challenging field of scientific research. Almost all the research outcomes however are limited to time domain data analysis. For instance, the A/F ratio excursion from stoichiometry (14.7) deteriorates the fuel economy, exhaust emissions and vehicle driveability. The time delay constant and fraction of injected fuel into engine cylinders are two parameters to model the wall wetting phenomenon, where the linear least square model has been applied to solve the engine transient fuel control problem in the time domain [9]. Engine idle speed stability control has been well-recognized as a complicated highly nonlinear problem in automotive industry. All existing classical, modern, and intelligent control theories have been applied to engine idle speed control. The two key control variables of the target idle speed and coolant temperature are both varying over the time [10]. Nonparametric frequency response identification via STFT is also presented to design robust linear controllers, together with the mixed sensitivity function optimization. It is applied to engine idle speed control using dynamometer testing. It generates much better delay margins. However its role in idle speed control is quite limited [11]. In order to optimize the overall performance of gasoline direct injection powertrain systems, both fuel economy and exhaust gas aftertreatment have to be taken into account. When the lean burn technology is employed to reduce fuel consumption, exhaust emission levels would increase on the other hand. Fuel injection control and exhaust emission control approaches are still dominated by the time domain data analysis [12-13]. In this preliminary study, time–frequency analysis of automotive engine performances will be conducted across diverse case studies. STFT has been applied by using the 3D spectrogram representation to reveal hidden properties beyond the classical time domain analysis.

2. Discrete time short-time Fourier transform (STFT)

In the discrete time domain, the transforming data sequence can be divided into overlapped frames. Fourier transform is carried out in each frame. The magnitude and phase for each point in time and frequency will be recorded. The complex spectrogram in each frame will be collected and formulated as a matrix. The discrete time STFT is expressed as (1).

$$X_n(\omega) = \sum_{m=-\infty}^{+\infty} x(m) W(m - nR) e^{-j\omega m} \quad (1)$$

where x(m) is the input signal sequence with the time index m; W(m) is the window function of the selected length M; R is the selected hop size between successive windows in samples; $X_n(\omega)$ is the discrete-time Fourier transform (DTFT) of the windowed data around the center time (nR), where DTFT is simply formulated as (2).

$$X(\omega) = \sum_{m=-\infty}^{+\infty} x(m) e^{-j\omega m} \quad (2)$$

The nature of STFT is determined by the shape of window functions. Typical window functions W(m) include the rectangular window, triangular window, Gaussian window, Chebyshev window, Hamming window, Hann window, Kaiser window, Blackman window, as well as the FlatTop window. The rectangular window produces the narrowest bandwidth which is seldom used in practice due to the leakage effect. The FlatTop window and the Hamming window will generate the largest and smallest bandwidth in practical implementation, respectively. In case that critical temporal features and fast frequency modulation are needed, wide bandwidths should be applied (e.g. FlatTop window). Conversely narrow bandwidths should be applied to focus on those frequency features (e.g. Hamming window).

The spectrogram is the visual representation of the signal strength in terms of the frequency spectrum. It is formulated as the magnitude squared of the STFT in (3), which is relevant to the power spectral density of the function. A narrow-band spectrogram corresponds to the long length M of the window frame, while a wide-band spectrogram in turn corresponds to the short length M of the window frame. Each spectrogram covers the list of amplitudes of the window frame size. The kth amplitude is associated with the actual frequency k.

$$Spectrogram = | X_n(\omega) |^2 = | STFT(x, W) |^2 \quad (3)$$

STFT computation can be conducted via M-point fast Fourier transform (FFT) in each window frame. Each window frame has to be zero-padded to avoid aliasing effects. Thus (M-R) zeros will be padded at the end of input signal sequence via zero-padding. In fact the FFT stems from discrete Fourier transform (DFT), which is regarded as a special case of the DTFT for finite causal signals. The M-point DFT is defined as (4), where W_M represents the M-th root of unity in (5).

$$X(i) = \sum_{k=0}^{M-1} x(k) W_M^{ik} \quad (0 \le i < M) \tag{4}$$

$$W_M = e^{-j2\pi/M} \tag{5}$$

The simplest FFT scheme is to split the M-point data sequence into two separate (M/2)-point data sequences in terms of the even number and odd number, which is $(M/2)/\log_2(M)$ times faster than DFT.

$$\begin{aligned} X(i) &= \sum_{k=0}^{M/2-1} x(2k) W_M^{2ki} + \sum_{k=0}^{M/2-1} x(2k+1) W_M^{(2k+1)i} \\ &= \sum_{k=0}^{M/2-1} x_e(k) W_{M/2}^{ki} + W_M^i \sum_{k=0}^{M/2-1} x_o(k) W_{M/2}^{ki} \\ &= DFT\{x_e(k)\} + W_M^i DFT\{x_o(k)\} \quad (0 \le i < M) \end{aligned} \tag{6}$$

Without loss of generality, being a generalized cosine window, numerical simulations with respect to the Blackman window ($a_0 = 0.42$, $a_1 = 0.5$, $a_2 = 0.08$) has been selected in the following sessions via the (M/2) point FFT scheme.

3. Idle speed stability comparisons between 2 typical engines

When the engine is idling, a target rotational speed has to be maintained in order to keep running without stalling out. The automotive engine idle speed could range from 600 rpm to 1000 rpm. The low engine idle speed is helpful to reduce fuel consumption, but meanwhile it can also generate stability problems. The goal of engine idle speed control is to stabilize and smooth the engine at the low idle speed against various uncertainties and external loads such as cylinder to cylinder variations, air conditioner, power steering, AC alternator and water pump.

In this session, time–frequency analysis of automotive engine idle speed stability is presented. Two typical 4-cylinder engines for the luxury vehicle (Mercedes) and economy vehicle (Ford) are selected for comparison purposes. Rather than measuring the engine speed along with time, some experiments are conducted to collect the audio signals at engine startup and at steady state of idling. For each engine, it is convenient to measure the audio signals in two diverse cases of startup and idling. After normalization, 2 sets of time domain signals are plotted in Figure 1, together with the related zero crossing rates, which is the simple means to describe the smoothness of the idle speed quality using the number of zero-crossings within a time window being applied. Obviously the idle speed quality at the steady state should be much smoother than that during the quick startup. The focus of the context, however, is to extract some features in the frequency domain, such that other properties can be captured using time–frequency analysis on idle speed quality. Accordingly discrete time STFT is employed where outcomes from multiple cases could compare with each other to reveal hidden characteristics based on 3D spectrogram plots, covering cases of both startup and steady states of idling for two engines from the luxury and economy vehicles.

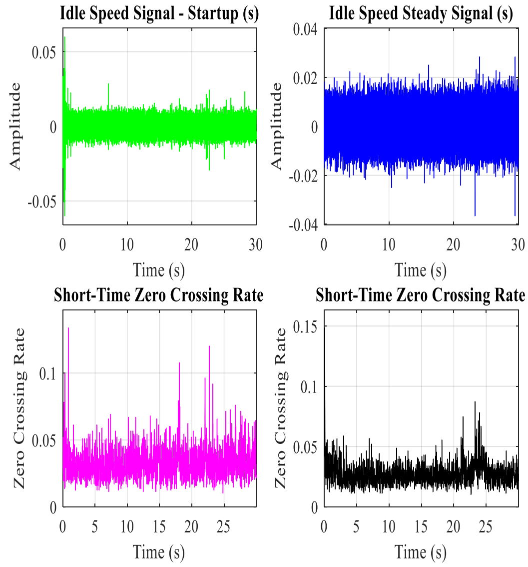

Figure 1: Engine idle speed signals and zero crossing rates during startup and steady state

In Figure 2, the window frame and hop size being adopted are 1024 and 512 sample points, respectively. 3D spectrogram is mostly depicted as a heat map based on a decibel scale (dB) of the intensity. All intensity values will be described by the false color. For example, red color is much stronger than blue color in dB. During the engine startup, the magnitude of the case B on the right (luxury engine) is much less than that of the case A on the left (economy engine), indicating that the luxury engine being tested runs at relatively low idle speed, which will benefit fuel economy. On the other hand, the frequency variation of the case B (luxury engine) is much higher than that of the case A (economy engine). It indicates that during the transient process, control algorithms and commands delivered by an Engine Electronic Unit (ECU) of the luxury engine plays the better role than those of the economy engine. In the steady state of engine idling, the magnitude of the case B (luxury engine) is still much less than that of the case A (economy engine), manifesting that the luxury engine being tested requires the relatively low idle speed, which will benefit fuel economy. Conversely however, the frequency variation of the case B (luxury engine) is much smaller than that of the case A (economy engine). It indicates that during the steady state of engine idling, the luxury engine produces the smoother idle speed operation than the economy engine.

When two 4-cylinder engines of the luxury vehicle (Mercedes) and economy vehicle (Ford) with the same displacement are chosen, based on time–frequency analysis of engine idle speed stability issues at both the transient state and steady state, it can be found out that the luxury engine being tested operates at relatively lower idle speed but runs smoother than the economy engine. As a result, the luxury engine requires the fewer amount of fuel consumption but it provides more comfortable condition during idling. In Figure 3, the window frame and hop size have been switched to 512 and 256 sample points, respectively. The conclusions being drawn are actually the same. Thus in all subsequent sessions being discussed, resolutions in time domain and frequency domain will be no longer emphasized.

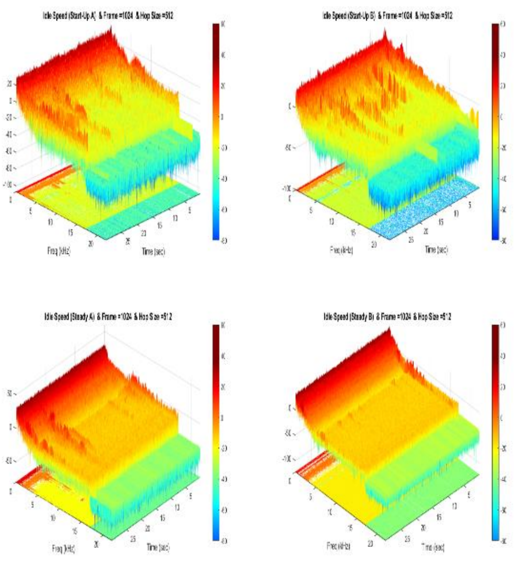

Figure 2: Comparisons of 3D spectrogram plots on idle speed quality (Case 1)

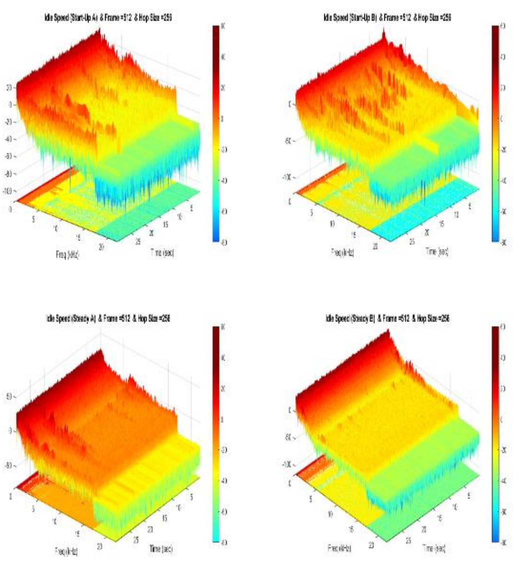

Figure 3: Comparisons of 3D spectrogram plots on idle speed quality (Case 2)

4. Time–frequency analysis of the air/fuel ratio in lean burn engine

The fuel economy of an internal combustion engine can benefit from the lean burn technology. The A/F ratio is the mass ratio of air to fuel in an engine combustion process. The A/F ratio in the stoichiometric mixture is defined as 14.7 (stoichiometry). When the A/F ratio is lower than the stoichiometry, the rich air fuel mixture is formed. When the A/F ratio is higher than the stoichiometry, the lean air fuel mixture is formed. Lean burn simply means the burning of fuel with an excess of air inside the combustion chamber.

The rich air fuel mixture gives rise to incomplete combustion inside. The incomplete combustion also results in the low combustion temperature, thus it leads to low levels of NOx. At the same time, however, extra amounts of CO and HC will be generated. On the other hand, the lean air fuel mixture corresponds to the excess air. The excess air in a lean-burn engine in turn will emit much less amount of CO and HC. The complete combustion with the sufficient amount of oxygen leads to the high combustion temperature over time, thus it produces high levels of NOx.

It is clearly shown that the A/F ratio plays a dominant role in the fuel economy, amount of exhaust emissions (NOx, CO and HC) as well as the power output. In this case, it is necessary to conduct time-frequency analysis of the A/F ratio in lean burn engines. For the exhaust aftertreatment system of lean burn engines, the Lean NOx Trap (LNT) is required to manage the amount of NOx. Because the LNT has its maximum capacity limit. Periodic NOx storage (lean burn) and NOx purge (rich burn) cycles are necessary (e.g. storage: 60 sec and purge: 2-3 sec in each cycle).

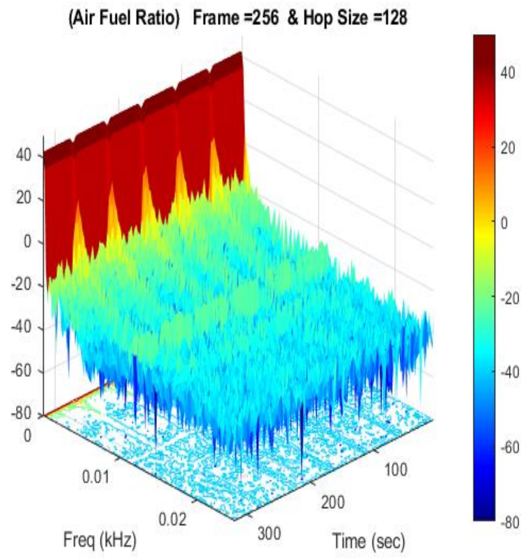

Figure 4: 3D spectrogram plots of A/F ratio data in lean burn technology

In Figure 4, the window frame and hop size have been selected as the 256 and 128 sample points, respectively. The data are collected from the 6-cylinder Ford engine using lean burn technology. In the time domain, A/F ratio is generally higher than the stoichiometry with lean burn technology, except for periodically switching to rich air fuel mixture for a very short time during the purge mode in each cycle. In the frequency domain, it shows that high A/F ratio (lean burn) corresponds to the relatively low frequency. It indicates that a majority of engine operations in each cycle are conducted during lean combustion, which is mostly associated to the steady state operation. The low A/F ratio (rich burn) instead corresponds to the relatively high frequency. It indicates that a minority of engine operations in each cycle are conducted at incomplete rich combustion, which is mostly associated to transient state operation. In addition, between the relatively low frequency and relatively high frequency, the transition of the A/F ratio along the frequency coordinate gives rise to a sharp slope across the transition band. It is relevant to the fact that the operating mode switching occurs twice in any single cycle, from lean burn to rich burn, or conversely from rich burn to lean burn.

5. Time–frequency analysis of the exhaust gas emission levels

In Figure 5, the window frame and hop size cover 256 and 128 sample points, respectively. The data (HC, CO, NOx, O_2) are still collected from 6-cylinder Ford engine with the lean burn technology, using diverse types of sensors (e.g. oxygen sensors). The goal of exhaust gas aftertreatment is to significantly improve the air quality and avoid pollution. HC, CO and NOx are typical exhaust emissions on which the control algorithms are focusing. The formation mechanisms vary case by case across different types of emissions. Tradeoff is always needed in the exhaust emission control system. For example, the incomplete combustion leads to the low combustion temperature, it generates excessive amount of CO and HC emissions, however in turn it helps to reduce the amount of the NOx emission at the same time.

In the time domain, similar pattern occurs periodically for every emission curves when switching between lean air fuel mixture in the NOx storage mode and rich air fuel mixture in the purge mode across each cycle. In the frequency domain, the highest amounts of HC, CO and NOx emission levels all correspond to the relatively low frequency, which belongs to the relatively steady operating mode. The lowest amounts of the HC, CO and NOx emission levels instead all correspond to the relatively high frequency, which are associated with the transient engine operating period, at the expense of extra control actions being needed. There are a couple of local peak values along the frequency coordinates in each case of HC, CO and NOx when time coordinates are fixed. In fact these peak values are associated with system responses of sudden switching between lean burn and rich burn. It shows that the instantaneous responses to the operating mode switching control action actually lead to additional amounts of exhaust emissions. Furthermore, in the frequency domain, the highest amount of oxygen levels also correspond to the relatively low frequency, which turns out to be the lean mode (e.g., 60 seconds duration). The lowest amount of oxygen levels instead corresponds to the sudden purge operation in the rich mode (e.g., 2-3 seconds duration). There are still a couple of local peak values of the oxygen level along the frequency coordinates when the time coordinates are fixed. These peak values are actually related to instantaneous responses to sudden engine operating mode switching between the lean burn and rich burn, which can not be directly observed based on the simple time domain analysis exclusively.

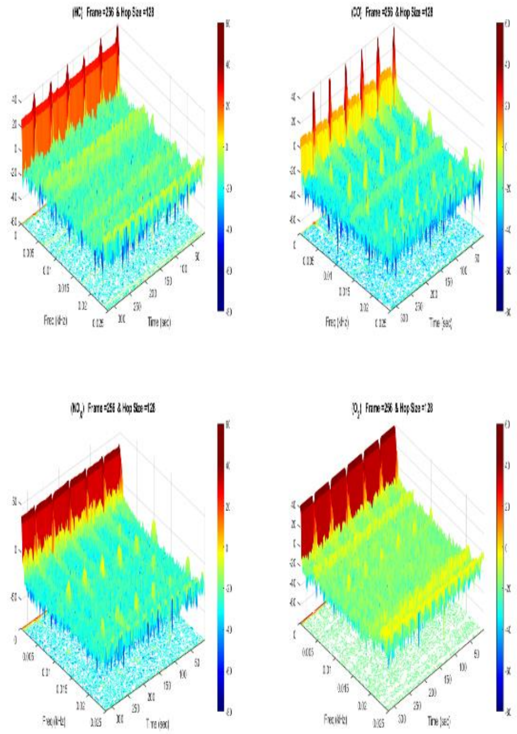

Figure 5: 3D spectrogram of exhaust emission levels (1) HC; (2) CO; (3) NOx; (4) O_2

It has been demonstrated from all three cases of engine performance analyses that the time-frequency approach has superiority over the exclusive time domain analysis. Some special latent characteristics have been discovered via the frequency domain analysis on a basis of STFT. STFT turns out to be a promising approach, which can also be easily expanded to data analysis of all other aspects of automotive engine performance in the similar and straightforward way.

6. Conclusions

The short-time Fourier transform (STFT) analysis approach has been well implemented in automotive engine performance analysis in this study. The time–frequency approach via STFT has been applied to idle speed stability analysis, A/F ratio control and exhaust emission aftertreatment in terms of amounts of HC, CO, NOx and O2. All these systems are essentially highly nonlinear. In particular, the 3D spectrogram has been introduced for data analysis by visually representing the spectrum of frequencies when the data vary along with time. In this case, characteristics of engine performances have been well illustrated from different aspects in both the time and frequency domains, which is superior to the classical time domain analysis approach. All 3 cases of engine performance analyses have provided convincing results. The time–frequency analysis being proposed could also be easily extended to evaluate any other potential automotive engine systems being examined, such as the engine timing systems, combustion systems, vibration and balancing systems and exhaust emission systems. Except for the control application to enhance idle speed stability, the STFT scheme could also be further expanded to improve the quality of electronic throttle control, engine ignition control, fuel injection control, emission control, engine combustion control and engine vibration control, based on both time domain and frequency domain points of view. It points out the challenging direction of future works.

7. References

[1] H. Djurović, V. Popović, M. Simeunović, "The STFT-Based Estimator of Micro-Doppler Parameters", IEEE Transactions on Aerospace and Electronic Systems, v 53, n 3, pp. 1273-1283, June 2017

[2] D. Herr, D. Tahmoush, "Data-Driven STFT for UAV Micro-Doppler Signature Analysis", Proceedings of 2020 IEEE International Radar Conference, pp. 1023-1028, 2020, Florence, Italy

[3] A. Maqsood, D. Oslebo, K. Corzine, L. Parsa, Y. Ma, "STFT Cluster Analysis for DC Pulsed Load Monitoring and Fault Detection on Naval Shipboard Power Systems", IEEE Transactions on Transportation Electrification, v 6, n 2, pp. 821-831, June 2020

[4] S. Pei, S. Huang, "STFT with Adaptive Window Width Based on The Chirp Rate", IEEE Transactions on Signal Processing, v 60, n 8, pp. 4065-4080, Aug 2012

[5] W. Zhang, Y. Xiao, S. Sun, and H. Zhang, "Blind Separation of Closely-Spaced Multipath Signals Using an STFT-MUSIC Algorithm", Proceedings of the 15th IEEE International Conference on Signal Processing, Dec 6-9, 2020, Beijing, China

[6] S. Kumawat, M. Verma, Y. Nakashima, S. Raman, "Depthwise Spatio-Temporal STFT Convolution Neural Networks for Human Action Recognition", IEEE Transactions on Pattern Analysis and Machine Intelligence, 2021

[7] E. Cabal-Yepez., A. Garcia-Ramirez, R. Romero-Troncoso, A. Garcia-Perez, and A. Osornio-Rios, "Reconfigurable Monitoring System for Time-Frequency Analysis on Industrial Equipment through STFT and DWT", IEEE Transactions on Industrial Informatics, v 9, n 2, p 760-771, May 2013

[8] Z. Ye, H. Yin, R. Belu, H. Mohamadian, H. Cao, and Y. Ye, "Discrete Wavelet Denoising via Kernel Based Nonlinear Component Analysis: Case Studies", Proceedings of the 2021 IEEE Colombian Conference on Communications and Computing, May 26-28, 2021, Cali, Columbia

[9] Z. Ye, "A Simple Linear Approach for Transient Fuel Control", SAE Technical Paper Series 2003-01-0360, SAE Special Publications SP-1749, Electronic Engine Controls, March 3-6, 2003, SAE World Congress, Detroit, Michigan, USA

[10] Z. Ye, "Modeling, Identification, Design and Implementation of Nonlinear Automotive Idle Speed Control Systems - An Overview", IEEE Transactions on Systems, Man and Cybernetics: Applications and Reviews, Vol. 37, No. 6, pp. 1137-1151, 2007

[11] S. Zhao, A. Abass, A. Shenton, "Nonparametric Design of Robust Linear Controllers and Their Experimental Application to Idle Control", Proceedings of 2009 IASTED International Conference on Control and Applications, pp. 121-128, 2009

[12] Z. Ye, "GDI Engine Exhaust Aftertreatment System Analysis and Oxygen Sensor Based Identification, Modeling & Control of Lean NOx Trap", Proceedings of the 2003 ASME Internal Combustion Engine Division Spring Technical Conference, pp. 713-719, May 11-14, 2003, Salzburg, Austria

[13] Z. Ye, and L. Li, "Control Options for Exhaust Gas Aftertreatment and Fuel Economy of GDI Engine Systems", Proceedings of the 2003 IEEE International Conference on Decision and Control, pp. 1783-1788, Dec. 9-12, 2003, Maui, Hawaii, USA

[14] R. Schilling, S. Harris, "Fundamental of Digital Signal Processing Using Matlab", 3rd Edition, Cengage Learning, 2017

[15] R. Duda,P. Hart,D. Stork, "Pattern Classification", 2nd Edition, John Wiley & Sons, 2000

[16] R. Gonzalez and R. Woods, "Digital Image Processing", 3rd Edition, Prentice-Hall, 2008